

Gold surface with gold nitride—a surface enhanced Raman scattering active substrate

A. C. Brieva,^{1,a)} L. Alves,¹ S. Krishnamurthy,^{1,2} and L. Šiller^{1,b)}

¹*School of Chemical Engineering and Advanced Materials, Newcastle University, NE1 7RU Newcastle upon Tyne, United Kingdom*

²*School of Physical Sciences, Dublin City University, Dublin 9, Ireland*

(Received 16 September 2008; accepted 15 January 2009; published online 4 March 2009)

The nitration of gold surfaces is a nonpolluting method, which can lead to large scale production of substrates with remarkable properties and applications. We present a topographical study of the nanoscale structure of the gold nitride surfaces produced by radio frequency (rf) nitrogen plasma etching of thin gold films. Atomic force microscopy images taken after rf etching reveal the striking appearance of the cluster assembly with large clusters surrounded by small clusters (7.9 ± 1.4 and 2.3 ± 0.9 nm, respectively) appearing to exhibit an attractive interaction. We discuss the possible mechanism for this attraction based on a colloid model by Messina *et al.* [Phys. Rev. Lett. **85**, 872 (2000)]. This surface exhibits a notable surface enhanced Raman scattering effect demonstrated with L-alanine and rhodamine-6G. The significance of this work is that we found that this SERS active gold nitride surface can be prepared in just one step: by nitrogen plasma etching a thin gold film. Until now most SERS active gold cluster covered surfaces have been prepared in several steps very often requiring complex lithography. © 2009 American Institute of Physics.

[DOI: [10.1063/1.3082871](https://doi.org/10.1063/1.3082871)]

I. INTRODUCTION

Binary nitrides possess a variety of interesting features, such as high hardness, chemical stability, and possess useful magnetic and electrical properties, which made them suitable for a number of applications. Noble metals (i.e., Ru, Rh, Pd, Ag, Os, Ir, Pt, and Au) were not considered to form nitrides and so most work reporting the synthesis of noble metals nitrides only appeared in recent years.^{1–3} Gold nitride was initially synthesized² by irradiating a single crystal Au (110) surface with low energy nitrogen ions in an ultrahigh vacuum (UHV) environment. Photoemission spectroscopy^{4,5} identified two different chemically bonded species. Moreover, gold nitride species have been found in the gas phase: Drenck *et al.*⁶ observed the formation of nitrogen-gold AuN_n^- anions and dianions.

In addition to the irradiation of single crystal samples with nitrogen ions in UHV,^{2,4} gold nitride films have been formed by reactive ion sputtering,^{5,7} by radio frequency plasma etching (rf-etching)^{5,7,8} by reactive pulsed laser deposition,⁹ and plasma assisted physical vapor deposition using pulsed arc discharge.¹⁰ Work by Šiller *et al.*⁵ has shown that gold films with gold nitride display promising properties: they are harder than gold coatings while retaining a high electrical conductivity. Furthermore, these nitride-containing films are also sensitive to electron beam irradiation, indicating that x-ray or electron beam lithography may be used to directly write patterns on a gold nitride surface.¹¹

In this article we present a topographical study of gold

nitride surfaces produced by rf etching using atomic force microscopy (AFM) and we discuss a possible mechanism for formation for the observed topography. Raman scattering measurements demonstrate that the rf etched gold nitride surface is a surface enhanced Raman scattering (SERS) active substrate.

There are numerous methods for producing SERS active substrates. Currently, to obtain suitably “rough” noble metal surfaces lithography with direct writing, such as e-beam lithography in combination with evaporation is employed,¹² or, alternatively, aggregated silver or gold colloids from solutions are used. Other reported approaches are based upon etching, such as wet chemical etching of Cu with HNO_3 ,¹³ selective chemical etching¹⁴ or etching of graphite and then subsequent evaporation of gold on the roughened surface.¹⁵ However, these techniques are more complex than the nitrogen plasma etching approach that we report here and are likely to yield surfaces with higher levels of residual contamination.

II. EXPERIMENTAL

Gold films $\sim 1 \mu\text{m}$ thick were deposited in an argon atmosphere on standard 3 in. silicon wafers, with a 400 nm thermal oxide, using an Edwards AUTO500 magnetron sputtering system. The wafers were transferred to a plasma etching system (STS, BOC Edwards sputter system) and exposed to 13.56 MHz rf nitrogen plasma for about 30 min. The power employed to generate the plasma was 300 W and the target was biased to -240 V .⁷ During this process, the nitrogen pressure in the plasma chamber was 8.3 mbar and the flow rate of N_2 was $50 \text{ cm}^3/\text{s}$.⁷ A scanning probe microscope (Digital Instruments Inc., MultiMode), operated as an AFM in tapping mode, was used to investigate the evolution

^{a)}Author to whom correspondence should be addressed. Electronic mail: abel.brieva@ncl.ac.uk.

^{b)}Author to whom correspondence should be addressed. Electronic mail: lidja.siller@ncl.ac.uk.

of the morphology of the etched surface. The presence of gold nitride was confirmed by photoemission and has been published elsewhere.⁵ For the Raman measurements of L-alanine, a WiTec CRM-200 Raman microscope was used with a He-Ne laser ($\lambda=632.8$ nm) excitation source. The rhodamine-6G spectra were taken with a Jobin Yvon HR800 Raman microscope using an argon laser ($\lambda=514.5$ nm) as the excitation source. L-alanine (>99.5% purity Fluka Bio-Chemika) in aqueous solution with a concentration of 5×10^{-4} mol/l, close to physiological values and rhodamine-6G (83697 Fluka BioChemika) in ethanol at 10^{-6} mol/l were used as analytes. As a preconcentration treatment we used the so called drop coating deposition Raman (DCDR) method,¹⁶ probing with the Raman microscope on the solid deposits left by the evaporation of a drop of the solution. This method introduces no unevenness between different points of the sample¹⁷ and the preconcentration of the analyte makes the Raman analysis possible. In order to achieve good reproducibility in the Raman measurements, we used long acquisition times (from 20 to 30 min in the L-alanine experiments and from 1 to 2 min with the rhodamine-6G). We observed good uniformity across the substrate under the experimental conditions described. The intensities of Raman bands fluctuate in SERS measurements due to the small number of molecules from which the signal originates.^{18,19} In a separate series of Raman experiments (not presented here) with acquisition times of only 5 s and using no preconcentration treatment (i.e., without the DCDR method), we observed strong intensity fluctuations in the Raman bands typical of SERS measurements.

To evaluate the Raman scattering from the gold nitride substrate, a comparison experiment was performed by undertaking a series of identical measurements on monocrystalline undecane-terminated Si(111) wafers, the hydrophobic surface of which is also suitable for the DCDR method.¹⁷ The flatness of the silicon surfaces was checked by AFM. Prior to DCDR deposition, in order to eliminate any contamination both substrates were rinsed with anhydrous ethanol (Sigma-Aldrich 459863).

III. RESULTS AND DISCUSSION

Figures 1(a) and 1(b) show two topographic views of the gold surface with gold nitride after rf nitrogen etching. The formation of large and small clusters on the surface is observed, with the majority of the smaller clusters appearing to surround the larger clusters. An image of one of the large clusters surrounded by small clusters is shown in Fig. 2. We obtained the cluster size from the height measurements. Throughout the entire set of images the height measurements were performed which gave height distributions of 7.9 ± 1.4 and 2.3 ± 0.9 nm for the larger and smaller clusters, respectively.

The possibility of attraction between two like-charged colloidal spheres (“macroions”) is still a central issue in colloidal science today,²⁰ with many experimental observations of attractions reported in the presence of confined surfaces,^{21–24} as well as without confinement.²⁵ However, the detailed mechanism of the attractions remains unknown. All

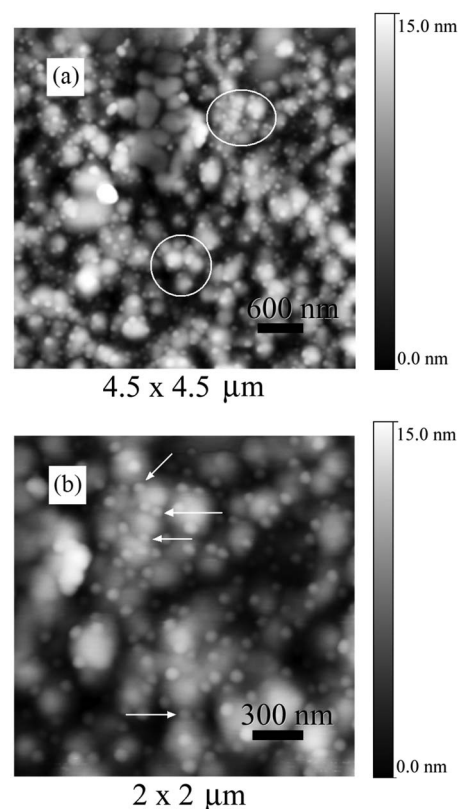


FIG. 1. AFM images showing the topography of the surface of thin gold films after rf-etching with nitrogen, which illustrates some examples of (a) the grouping of macroions and (b) sharing of counterions by contiguous macroions.

experiments on confinement-induced attraction were performed on polystyrene microspheres with highly acidic surface groups.^{21–24} Several theoretical models have been proposed^{26–29} to explain this behavior. Here in this work, we present experimental evidence that the model of the counterion-macroion system²⁶ is likely to be responsible for an effective attraction of like-charged macroions near confined surfaces. We provide experimental evidence on confinement-induced attraction within the plasma with aggregated particles landing subsequently on the surface. Electrostatic correlations play an important role in plasmas because they result in thermodynamic instability and phase separation.²⁰

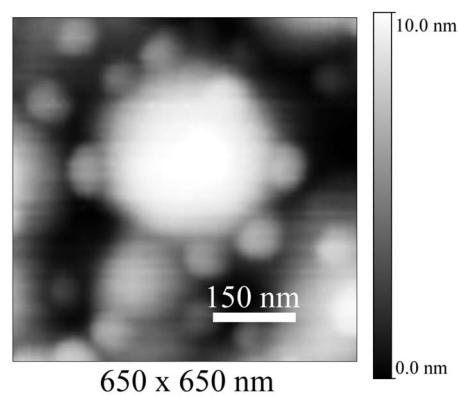


FIG. 2. AFM image of one of the macroions surrounded by counterions.

From Fig. 1(a) it is clear that these decorated islands are not just arbitrarily distributed over the surface, but coalesce to form island groups [see circled areas in the image in Fig. 1(a)], indicating that there is an attractive force between them. This distribution is strongly reminiscent of the predicted behavior of counterions and macroions in colloidal systems,²⁶ consistent with a possible liquidlike behavior on the film surface during plasma treatment (during rf etching the ions and charged sputtered gold clusters from the plasma cannot be easily neutralized because the substrate has a 400 nm thick SiO_x layer, see discussion below). The Messina model²⁶ predicts that two highly charged macroions separated by intermediate distances and surrounded by counterions can experience a long range Coulomb attractive force [as observed in Fig. 1(a)] and thus can group together due to the presence of metastable ionized states. It has been suggested²⁶ that these states occur when small changes due to thermal fluctuation in a highly charged colloid distribute the counterions unevenly, leading to one overcharged and one undercharged macroion.

In order to explain the phase separation and to understand the possible origin of the attraction, it is necessary to review the experimental conditions. The thin gold film, $\sim 1 \mu\text{m}$ thick, deposited on a Si wafer with a thick oxide layer (400 nm thick), has been exposed to rf nitrogen plasma etching at 13.56 MHz. In each half of the cycle—when the surface is struck with electrons—the gold film becomes negatively charged due to the presence of the thick oxide layer on the wafer. The positive nitrogen ions from the plasma will be attracted toward the surface and will partially remove gold (some clusters of gold are expected to be removed). However these gold clusters cannot move very far from the surface because they quickly become positively charged in the nitrogen plasma and as such become “counterions” (most likely in the form of a gold nitride). In the alternate plasma-etching cycle these “gold nitride counterions” further attach to the negatively charged gold surface, forming macroion-counterion complexes. These complexes will experience attraction because the overall negative charge of the gold macroions is screened by the counterions present, resulting in the attractive interaction predicted by Messina *et al.*²⁶

We suggest that the arrangement observed [Figs. 1(a) and 1(b)] of the counterions surrounding the macroions is the result of a transient process, with a definite time of relaxation, which takes place during the landing of the counterions on the gold film, and during that process the counterions could arrange themselves. The native silicon oxide beneath the gold layer may play an important role in such a process, since it stops the flow of the charge.³⁰ During the half cycle in which the ion bombardment occurs the gold layer becomes increasingly positively charged, weakening and eventually canceling out the electric force, which drives the counterions into the gold substrate, giving this process the necessary time of relaxation and allowing the macroions to move around the surface. This charging effect would stop the etching process, but during the opposite half cycle, the charge is removed and the structures formed become permanent. The image [Fig. 1(a)] is indirect evidence of the forma-

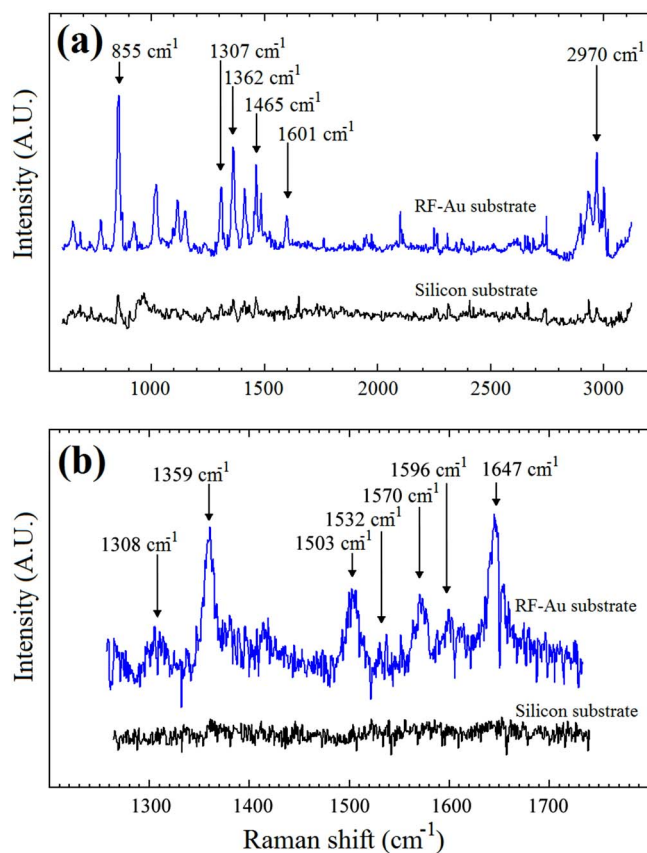


FIG. 3. (Color online) (a) Raman spectra of 5×10^{-4} mol/l aqueous solution of L-alanine deposited on rf-etched gold and silicon hydrophobic substrates using the DCDR method (Ref. 17). The acquisition time was 20 min in both cases. (b) The same experiment was performed using rhodamine-6G as analyte in ethanol solution 10^{-6} mol/l, the acquisition time was 2 min.

tion of macroion-counterion complexes and in Fig. 1(b) we show, as denoted by the arrows, that counterions can be shared between two macroions (as additional evidence of the attraction). Thus this interpretation is in agreement with the theoretical model²⁶ where the attraction between the two macroion-counterion complexes has been achieved due to imbalance of the counterion charge.

SERS was observed initially³¹ and characterized³² on roughened noble-metal surfaces. Over the past three decades, theoretical modeling provided an insight into electromagnetic enhancement on surfaces containing noble-metal nanoparticles (e.g., Refs. 33 and 34). In order to probe the possible SERS activity of the rf etched gold, a series of Raman experiments were conducted. Figure 3(a) shows Raman spectra from a 5×10^{-4} mol/l aqueous solution of L-alanine prepared by the DCDR method¹⁶ on rf etched gold (top) and a hydrophobic undecane terminated silicon substrate (bottom). The bands that appear [Fig. 3(a), top] at Raman shifts of 855, 1307, 1362, 1465, 1601, and 2970 cm^{-1} are attributed to L-alanine.^{35,36} Only the feature at 855 cm^{-1} is (barely) visible in the spectrum taken on silicon [Fig. 3(a), bottom]. It is particularly noticeable that the broad feature at about 3000 cm^{-1} is completely indistinguishable on the silicon substrate. In the rhodamine-6G experiments (10^{-6} mol/l in ethanol), the bands assigned to rhodamine³⁷ observed at Raman shifts of 1308, 1359, 1503, 1532, 1570, 1596, and

1647 cm^{-1} [Fig. 3(b), top] are undetectable on the silicon substrate [Fig. 3(b), bottom]. Those experiments clearly demonstrate the SERS-active nature of the rf-etched gold surface. Similar results to those discussed above are obtained on substrates etched four years ago and stored in air ambient conditions, showing the high durability of the rf-etched surfaces.

IV. CONCLUSIONS

In summary, we present indirect experimental observation of the spherelike macroion-counterion assembly. We show that gold nitride rf etched surfaces are SERS active. The feasibility of the rf-etching process being applied to large areas makes this SERS active substrate a potentially useful material for technological and industrial applications.

ACKNOWLEDGMENTS

This work was supported by EPSRC (Grant no. EP/C006011/1). We thank Mr. P. R. Coxon for a critical reading of the manuscript.

- ¹J. C. Crowhurst, A. F. Goncharov, B. Sadigh, C. L. Evans, P. G. Morrall, J. L. Ferreira, and A. J. Nelson, *Science* **311**, 1275 (2006).
- ²L. Šiller, M. R. C. Hunt, J. W. Brown, J. M. Coquel, and P. Rudolf, *Surf. Sci.* **513**, 78 (2002).
- ³A. F. Young, C. Sanloup, E. Gregoryanz, S. Scandolo, R. J. Hemley, and H. K. Mao, *Phys. Rev. Lett.* **96**, 155501 (2006).
- ⁴S. Krishnamurthy, M. Montalti, M. G. Wardle, M. J. Shaw, P. R. Briddon, K. Svensson, M. R. C. Hunt, and L. Šiller, *Phys. Rev. B* **70**, 045414 (2004).
- ⁵L. Šiller, N. Peltekis, S. Krishnamurthy, Y. Chao, S. J. Bull, and M. R. C. Hunt, *Appl. Phys. Lett.* **86**, 221912 (2005).
- ⁶K. Drenck, P. Hvelplund, C. J. McKenzie, and S. B. Nielsen, *Int. J. Mass Spectrom.* **244**, 144 (2005).
- ⁷L. Šiller, S. Krishnamurthy, and Y. Chao, UK Patent No. GB 0413036.5, WO 2005/121395 (2005).
- ⁸L. Alves, T. P. A. Hase, M. R. C. Hunt, A. C. Brieva, and L. Šiller, *J. Appl. Phys.* **104**, 113527 (2008).
- ⁹A. P. Caricato, M. Fernandez, G. Leggieri, A. Luches, M. Martino, F. Romano, T. Tunno, D. Valerini, A. Verdyan, Y. M. Soifer, J. Azoulay, and L. Meda, *Appl. Surf. Sci.* **253**, 8037 (2007).
- ¹⁰A. Devia, H. A. Castillo, V. J. Benavides, Y. C. Arango, and J. H. Quintero, *Mater. Charact.* **59**, 105 (2008).
- ¹¹Y. V. Butenko, L. Alves, A. C. Brieva, J. Yang, S. Krishnamurthy, and L. Šiller, *Chem. Phys. Lett.* **430**, 89 (2006).
- ¹²D. Cialla, U. Hubner, H. Schneidewind, R. Moller, and J. Poop, *ChemPhysChem* **9**, 758 (2008).
- ¹³F. Li, Y. Lu, G. Xue, and G. Cao, *Chem. Phys. Lett.* **264**, 376 (1997).
- ¹⁴M. C. Dixon, T. A. Daniel, M. Hieda, D. M. Smilgies, M. H. W. Chan, and D. L. Allara, *Langmuir* **23**, 2414 (2007).
- ¹⁵J. V. Zoval, P. R. Biernacki, and R. M. Penner, *Anal. Chem.* **68**, 1585 (1996).
- ¹⁶D. M. Zhang, Y. Xie, M. F. Mrozek, C. Ortiz, V. J. Davisson, and D. Ben-Amotz, *Anal. Chem.* **75**, 5703 (2003).
- ¹⁷C. Ortiz, D. M. Zhang, Y. Xie, A. E. Ribbe, and D. Ben-Amotz, *Anal. Biochem.* **353**, 157 (2006).
- ¹⁸A. Kudelski, *Chem. Phys. Lett.* **414**, 271 (2005).
- ¹⁹S. M. Nie and S. R. Emery, *Science* **275**, 1102 (1997).
- ²⁰Y. Levin, *Rep. Prog. Phys.* **65**, 1577 (2002).
- ²¹J. C. Crocker and D. G. Grier, *Phys. Rev. Lett.* **77**, 1897 (1996).
- ²²Y. L. Han and D. G. Grier, *Phys. Rev. Lett.* **91**, 038302 (2003).
- ²³G. M. Kepler and S. Fraden, *Phys. Rev. Lett.* **73**, 356 (1994).
- ²⁴A. E. Larsen and D. G. Grier, *Nature (London)* **385**, 230 (1997).
- ²⁵K. Ito, H. Yoshida, and N. Ise, *Science* **263**, 66 (1994).
- ²⁶R. Messina, C. Holm, and K. Kremer, *Phys. Rev. Lett.* **85**, 872 (2000).
- ²⁷E. Allahyarov, I. D'Amico, and H. Lowen, *Phys. Rev. Lett.* **81**, 1334 (1998).
- ²⁸T. M. Squires and M. P. Brenner, *Phys. Rev. Lett.* **85**, 4976 (2000).
- ²⁹P. Linse and V. Lobaskin, *Phys. Rev. Lett.* **83**, 4208 (1999).
- ³⁰We performed test measurements where we used AFM to measure the topography of gold nitride formed by the plasma method when the surface of the gold nitride is in direct contact with a metal, "metal sample," and when it was completely insulated, we used a polyamide film as a substrate and deposited first the gold by argon sputtering, then we isolated the sample from any metal parts in the plasma chamber in order to etch the surface. We observed that the clusters produced on insulated sample are much smaller in size than on "metal" sample. We could not observe any of the features presented in this work on metal samples (data not presented here).
- ³¹M. Fleischmann, P. J. Hendra, and A. J. McQuilla, *Chem. Phys. Lett.* **26**, 163 (1974).
- ³²D. L. Jeanmaire and R. P. Vanduyne, *J. Electroanal. Chem.* **84**, 1 (1977).
- ³³T. Jensen, L. Kelly, A. Lazarides, and G. C. Schatz, *J. Cluster Sci.* **10**, 295 (1999).
- ³⁴H. X. Xu, *Appl. Phys. Lett.* **85**, 5980 (2004).
- ³⁵H. Susi and D. M. Byler, *J. Mol. Struct.* **63**, 1 (1980).
- ³⁶C. H. Wang and R. D. Storms, *J. Chem. Phys.* **55**, 3291 (1971).
- ³⁷J. Schwarz, C. Contescu, and K. Putyera, *Dekker Encyclopedia of Nanoscience and Nanotechnology* (Taylor & Francis, London, 2004), Vol. 4, p. 2698.